

# FREQUENCY-SHAPED RANDOMIZED SAMPLING

*Sourav R. Dey and Alan V. Oppenheim*

Massachusetts Institute of Technology  
Digital Signal Processing Group  
77 Massachusetts Avenue, Cambridge MA 02139  
*sdey@mit.edu, avo@mit.edu*

## ABSTRACT

This paper explores the use of discrete-time randomized sampling as a method to mitigate the effects of aliasing. Two distinct sampling architectures are presented along with second-order characterizations of the resulting sampling error. In the first, denoted simple randomized sampling, non-white sampling processes are shown to frequency-shape the error spectrum, so that its power is minimized in the band of interest. The design of non-white binary processes for use in randomized sampling is considered. In the second model, denoted filtered randomized sampling, a pre-filter, post-filter, and the sampling process are used to achieve a similar effect. In both cases, optimal mean-squared-error solutions are derived. Results from simulation are shown.

**Index Terms**— randomized sampling, non-uniform sampling, LTI reconstruction, noise-shaping

## 1. INTRODUCTION

Randomized sampling can be used as an effective technique to modify the impact of aliasing. With periodic sampling, if the input signal is sampled below its Nyquist rate, aliasing occurs. Though an anti-aliasing filter can be used, it imposes a severe restriction on the range of frequencies that can be represented. In addition, in certain applications, like ray-traced computer graphics, anti-aliasing filters are impossible to implement, [1]. With randomized sampling, the error due to undersampling corresponds approximately to wideband noise that is uncorrelated with the input signal, [2]. In perceptual applications such as audio and imaging, the distortion from this wideband noise is often preferable to aliasing artifacts, [3, 1, 4].

Most literature on randomized sampling considers a randomization of the sampling process in continuous-time [5]. By contrast, in this paper, randomized sampling is modeled as a discrete-time (DT) down-sampling process. The formulation follows the randomized down-sampling framework presented in [2]. In this paper, we extend the white randomized down-sampling models of [2] to non-white randomized down-sampling models which can further reduce the error due to undersampling.

The techniques presented in this paper have potential applications in contexts where there are limitations on an analog-to-digital converter (ADC). For example, in wideband surveillance, the maximum sampling rate of an ADC might be below the Nyquist rate for signals of interest. In this context, randomized sampling can be used to algorithmically extend the effective bandwidth of the ADC. As

another example, for low power applications such as sensor network nodes, sampling consumes a large portion of the power. In this case, randomized sampling can be used to reduce the sampling rate, and correspondingly the power consumption.

## 2. RANDOMIZED SAMPLING MODELS

For an LTI system with a wide-sense stationary (WSS) input,  $x[n]$ , and a deterministic impulse response,  $h[n]$ , DT randomized sampling is defined as the process of randomly setting some of the samples of  $x[n]$  to zero. In this paper, we consider two forms of DT randomized sampling. The first, denoted simple randomized sampling (SRS), does not incorporate pre and post-filtering as illustrated in Fig. 1(a). The second, denoted filtered randomized sampling (FRS), has a user-definable pre-filter and post-filter as illustrated in Fig. 1(b).

In both cases, randomized sampling is represented as multiplication with a binary WSS process,  $r[n] = \{1, 0\}$ , that is statistically independent of the input  $x[n]$ . The resulting DT signal is thus on the same sampling grid, but with many samples set to zero. Note that this model implicitly preserves knowledge of the sampling indices upon reconstruction. This is in contrast to a fully randomized scheme where the sampling indices are unknown at reconstruction.

The fixed LTI filter  $h[n]$  represents a frequency-dependent error weighting, denoting frequency bands of interest with high values and less important bands with low values. In certain contexts,  $h[n]$  can be interpreted as a reconstruction filter. For example, in audio and imaging,  $h[n]$  can represent a model of human perception. In other contexts, like multi-carrier communications,  $h[n]$  can be used to model frequency-dependent SNR requirements.

The average sampling rate is assumed to be fixed. Mathematically, this fixes the mean of  $r[n]$  to a particular value,  $E\{r[n]\} = \mu$ . Since  $r[n]$  is a binary process, this constrains the variance to be,

$$\sigma_r^2 = \mu(1 - \mu) \quad (1)$$

In addition, the input power spectrum,  $S_{xx}(\omega)$ , is assumed to be known a priori. This makes the randomized sampling process a form of data-dependent sampling, where an a-priori characterization of the signal of interest is used to tune the sampling.

In SRS, the goal is to design a non-white sampling process,  $r[n]$ , subject to certain constraints, such that the reconstruction  $\hat{y}[n]$  is as close as possible to  $y[n]$ , the desired output without randomized sampling.  $y[n]$  is defined as,

$$y[n] = \mu x[n] * h[n] \quad (2)$$

Note that to make a fair comparison,  $y[n]$  has been scaled by the mean,  $\mu$ , of the sampling process. This accounts for the loss of

---

This work was supported in part by the NDSEG Fellowship, Texas Instruments Leadership University Program, BAE Systems PO 112991, and Lincoln Laboratory PO 3077828.

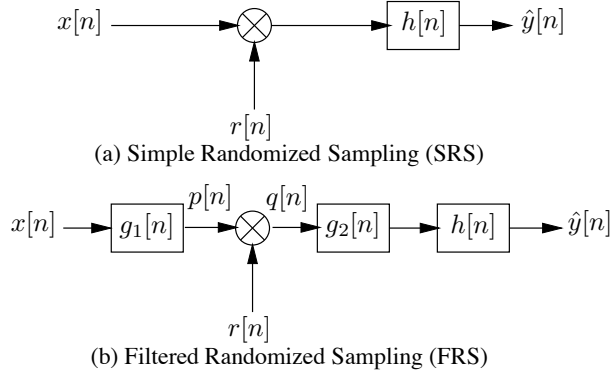


**Fig. 1.** Block diagrams for two models of randomized sampling.

energy due to sampling. The mean squared error (MSE), defined in Eqn.(3), is used as an error metric. Section 3 analyzes the SRS model in detail.

$$\mathcal{E} = E \{e^2[n]\} = E \{(y[n] - \hat{y}[n])^2\} \quad (3)$$

FRS is analogous to SRS, except that there are three design parameters, the pre-filter  $g_1[n]$ , the post-filter  $g_2[n]$ , and the sampling process  $r[n]$ . Section 4 analyzes the FRS model in detail.

### 3. SIMPLE RANDOMIZED SAMPLING

In SRS, the sampling process,  $r[n]$ , can be decomposed into the sum of its mean and a zero-mean random process,  $r_0[n]$ ,

$$r[n] = \mu + r_0[n] \quad (4)$$

where  $r_0[n] = \{(1 - \mu), -\mu\}$ . Using this decomposition, the output of randomized sampling can be expressed as,

$$z[n] = \mu x[n] + \underbrace{x[n]r_0[n]}_{w[n]} \quad (5)$$

Though  $w[n]$  is a function of  $x[n]$ , it is statistically uncorrelated with  $x[n]$ , i.e. the cross-covariance  $K_{xw}[m] = 0$ . The output,  $\hat{y}[n]$ , can be expressed as,

$$\hat{y}[n] = \mu y[n] + e[n] \quad (6)$$

where  $e[n] = w[n] * h[n]$ , a zero-mean additive error uncorrelated with  $y[n]$ . The PSD of  $e[n]$  can be expressed as,

$$S_{ee}(\omega) = |H(\omega)|^2 \left\{ \frac{1}{2\pi} \int_{-\pi}^{\pi} S_{xx}(\theta) \Phi_{rr}(\omega - \theta) d\theta \right\} \quad (7)$$

where  $\Phi_{rr}(\omega)$  is the covariance spectrum of  $r[n]$ . The integration corresponds to circular convolution with period  $2\pi$ . The MSE is found by integrating Eqn. (7),

$$\mathcal{E} = \frac{1}{4\pi^2} \int_{-\pi}^{\pi} \int_{-\pi}^{\pi} |H(\omega)|^2 S_{xx}(\theta) \Phi_{rr}(\omega - \theta) d\theta d\omega \quad (8)$$

In the randomized sampling model of [2], which we denote as white SRS,  $r[n]$  is assumed to be an IID Bernoulli process. In this model, the auto-covariance is  $K_{rr}[m] = \sigma_r^2 \delta[m]$  and the error power spectrum simplifies to,

$$S_{ee}(\omega) = \sigma_r^2 K_{xx}[0] |H(\omega)|^2 \quad (9)$$

The error thus has a flat power spectrum shaped by the filter  $h[n]$ .

### 3.1. Non-White SRS

By allowing correlations in  $r[n]$ , the error spectrum can be shaped so that its energy in the band of interest is reduced. Mathematically, the goal is to find  $\Phi_{rr}(\omega)$ , that minimizes the objective function Eqn.(8). There are three important constraints on  $\Phi_{rr}(\omega)$ . First,  $\Phi_{rr}(\omega)$  must be a valid covariance spectrum, i.e. real, non-negative, and symmetric. Secondly, since  $\mu$  is fixed, Eqn.(1) constrains the total area,

$$\frac{1}{2\pi} \int_{-\pi}^{\pi} \Phi_{rr}(\omega) d\omega = \sigma_r^2 = \mu(1 - \mu) \quad (10)$$

Furthermore,  $\Phi_{rr}(\omega)$  must be achievable by a binary process. Changing the order of convolution in Eqn.(8) the optimization can be formally defined as,

$$\min_{\Phi_{rr}(\omega)} \left\{ \frac{1}{4\pi^2} \int_{-\pi}^{\pi} \Phi_{rr}(\omega) F(\omega) d\omega \right\} \quad (11)$$

$$\text{where } F(\omega) = \int_{-\pi}^{\pi} |H(\theta)|^2 S_{xx}(\omega - \theta) d\theta$$

subject to Eqn.(10) and that  $\Phi_{rr}(\omega)$  can be achieved by a binary random process. Without the binary constraint, an optimal solution can be found, taking the form of two appropriately scaled impulses at  $\omega_0 = \arg \min_{\omega} F(\omega)$ ,

$$\Phi_{rr}(\omega) = 2\pi\sigma_r^2 \left( \frac{1}{2}\delta(\omega - \omega_0) + \frac{1}{2}\delta(\omega + \omega_0) \right) \quad (12)$$

Unfortunately, except in certain special cases, the power spectrum of Eqn.(12) cannot be achieved by a binary process. More generally, not all covariance spectra are achievable using binary processes. The set of achievable spectra has been studied in [6, 7]. Unfortunately, this set is not tractable for optimization.

### 3.2. Generating Binary Processes for SRS

The optimization of Eqn.(11) can be simplified by assuming a parametric model for  $r[n]$ . Though there are numerous techniques to generate binary processes, most do not give a tractable expression for the resulting covariance spectrum  $\Phi_{rr}(\omega)$ . Consequently, optimization for use in SRS is difficult.

A recent model, presented in [8], alleviates this problem. It can generate auto-regressive (AR) binary processes with a known covariance spectrum. The basic model is presented for completeness, for a more detailed description, the reader is referred to [8].

The AR binary process,  $r[n]$ , is generated iteratively from  $p$  previous samples,  $r[n-1], r[n-2], \dots, r[n-p]$  as follows,

1. The bias,  $r_b[n]$ , for the generation of  $r[n]$  is computed according to the relationship:

$$r_b[n] = \mu + \sum_{k=1}^p a_k (r[n-k] - \mu) \quad (13)$$

where  $\mu$  is the desired mean of  $r[n]$  and the  $a_k$  are parameters of the algorithm.

2. The sample  $r[n]$  is randomly generated from a binary distribution biased by  $r_b[n]$  as follows:

$$r[n] = \begin{cases} 1 & \text{with probability } r_b[n] \\ 0 & \text{with probability } 1 - r_b[n] \end{cases} \quad (14)$$

In steady-state, this process is wide-sense stationary with mean  $\mu$ . The auto-covariance spectrum can be shown to be auto-regressive, of the form,

$$\Phi_{rr}(e^{j\omega}) = \frac{A}{|H(e^{j\omega})|^2} = \frac{A}{|1 - \sum_{k=1}^p a_k e^{-j\omega k}|^2} \quad (15)$$

as long as the following constraint on the parameters  $a_k$  and  $\mu$  are satisfied:

$$\left( \sum_{k=1}^p a_k - 1 \right) > \frac{1}{|1 - 2\mu|} \left( \sum_{k=1}^p |a_k| - 1 \right) \quad (16)$$

This constraint ensures that there is no overflow in Eqn.(13), i.e. the bias,  $r_b[n]$  is bounded between 0 and 1, [8].

By substituting Eqn.(15) into Eqn.(11), fixing the number of parameters  $a_k$ , and imposing the constraint of Eqn.(16), numerical optimization can be used to solve for the optimal values of  $a_k$ . SRS using the resulting process  $r[n]$  will have MSE lower than white SRS, and in most cases, even lower than aliased uniform sampling. Section 5 illustrates an example of optimizing a two-pole binary AR process for use in SRS.

#### 4. FILTERED RANDOMIZED SAMPLING

FRS is an extension of SRS that incorporates a pre-filter and a post-filter. The filters offer extra degrees of freedom that can be used to further reduce the MSE. There are a number of possible FRS solutions, depending on the constraints imposed on the filters and the sampling process. In this paper, for the sake of brevity, we focus on one particular solution, denoted distortion-free white FRS (DFW-FRS).

##### 4.1. Distortion-Free White FRS

The DFW-FRS solution has two constraints. First, the sampling process,  $r[n]$ , is restricted to be white. Though non-white sampling processes could achieve a lower MSE, restricting  $r[n]$  to be white significantly simplifies the resulting optimization. In addition, white FRS gives an upper-bound on optimal FRS performance for non-white processes, much like white-SRS does for non-white SRS performance. Future work will address distortion-free FRS with non-white sampling processes.

Secondly, DFW-FRS imposes an invertibility constraint, where the filters  $g_1[n]$  and  $g_2[n]$  are constrained to be inverses of one another. This ensures that the error,  $e[n]$ , is unbiased and uncorrelated with the input, like in SRS. Mathematically, the output of the FRS system is,

$$\hat{y} = \mu(h * g_2 * g_1 * x) + h * g_2 * ((g_1 * x)r_0) \quad (17)$$

The dependence on  $n$  has been dropped for notational clarity. Collecting terms, the error,  $e[n] = y[n] - \hat{y}[n]$ , can be expressed as,

$$e = \underbrace{\mu(h * g_1 * g_2 - h)}_{u[n]} * x + \underbrace{h * g_2 * ((g_1 * x)r_0)}_{v[n]} \quad (18)$$

By choosing,

$$h[n] * g_1[n] * g_2[n] = h[n] \quad (19)$$

the term  $u[n] = 0$ . Consequently,  $e[n] = v[n]$ . Since  $E\{r_0[n]\} = 0$ , it is straightforward to show that  $E\{v[n]\} = 0$  and  $K_{vv}[m] = 0$ . The error is thus unbiased and uncorrelated with the input.

##### 4.2. Minimum MSE DFW-FRS Solution

Since  $r[n]$  is restricted to be a white process, i.e.  $K_{rr}[m] = \sigma_r^2 \delta[m]$ , defining  $p[n] = g_1[n] * r_0[n]$  and given the constraint of Eqn.(19), an expression for the error power spectrum can be derived directly from Eqn.(18) assuming  $e[n] = v[n]$ ,

$$S_{ee}(\omega) = \sigma_r^2 \sigma_p^2 |G_2(\omega)|^2 |H(\omega)|^2 \quad (20)$$

where  $\sigma_p^2$  denotes the variance of  $p[n]$ . It can be expressed as the area under  $S_{pp}(\omega)$ ,

$$\sigma_p^2 = \frac{1}{2\pi} \int_{-\pi}^{\pi} |G_1(\omega)|^2 S_{xx}(\omega) d\omega \quad (21)$$

In what follows,  $H(\omega)$  is assumed to be a non-invertible filter with a passband for  $|\omega| < \omega_p$  and a stopband for  $\omega_p < |\omega| < \pi$ .

By combining Eqns. (20) and (21), and incorporating the constraint of Eqn. (19), the MSE objective function can be expressed in the passband as an optimization over  $|G_1(\omega)|^2$ ,

$$\min_{|G_1(\omega)|^2} \sigma_r^2 \left( \int_{-\omega_p}^{\omega_p} |G_1(\omega)|^2 S_{xx}(\omega) d\omega \right) \left( \int_{-\omega_p}^{\omega_p} \frac{|H(\omega)|^2}{|G_1(\omega)|^2} d\omega \right) \quad (22)$$

with the understanding that  $G_1(\omega) = G_2(\omega) = 0$  in the stopband. Assuming that both integrands in Eqn.(22) are in  $\mathcal{L}_2(\omega_p)$ , the space of finite-energy sequences band-limited to  $\omega_p$ , the MSE can be bounded below using the Cauchy-Schwartz inequality,

$$\left( \int_{-\omega_p}^{\omega_p} |V_1(\omega)|^2 d\omega \right) \left( \int_{-\omega_p}^{\omega_p} |V_2(\omega)|^2 d\omega \right) \geq \left| \int_{-\omega_p}^{\omega_p} V_1^*(\omega) V_2(\omega) d\omega \right|^2 \quad (23)$$

This lower bound is met with equality if and only if  $V_1(\omega) = \alpha V_2(\omega)$ . Applying this relation to the integrands in Eqn.(22), the optimal filters are,

$$|G_1(\omega)|^2 = \alpha \frac{|H(\omega)|}{\sqrt{S_{xx}(\omega)}} \quad (24)$$

$$|G_2(\omega)|^2 = \frac{1}{\alpha} \frac{\sqrt{S_{xx}(\omega)}}{|H(\omega)|} \quad (25)$$

up to a scale factor  $\alpha$ . From the Cauchy-Schwartz inequality, the minimum MSE is,

$$\mathcal{E} = \sigma_r^2 \left( \int_{-\omega_p}^{\omega_p} \sqrt{S_{xx}(\omega)} |H(\omega)| d\omega \right)^2 \quad (26)$$

A non-trivial solution exists because  $G_1(\omega)$  is coupled to  $G_2(\omega)$  through the constraint of Eqn.(19). Otherwise the error could be made arbitrarily small by scaling  $G_2(\omega)$ . The fact that  $|G_1(\omega)|^2 = 1/|G_2(\omega)|^2$  amplifies the total error. These two competing effects minimize each other when the spectral shapes are chosen as Eqns.(24) and (25). Section 5 illustrates an example of DFW-FRS.

## 5. NUMERICAL EXPERIMENTS

In the following MATLAB simulations, we assume perfect knowledge of  $S_{xx}(\omega)$ . In practice of course, the power-spectrum of the input must be estimated from measurements or derived using prior information. The process  $x[n]$  is simulated by shaping white Gaussian noise through a filter,  $S(z)$ ,

$$S(z) = \frac{(z - z_0)}{(z - p_1)(z - p_1^*)(z - p_2)(z - p_2^*)} \quad (27)$$

where  $z_0 = 0.98$ ,  $p_1 = 0.9e^{j\pi/8}$ , and  $p_2 = 0.9e^{j3\pi/8}$ . The power spectrum is  $S_{xx}(\omega) = S(z)S(z^{-1})$ . The reconstruction filter,  $H(\omega)$ , is a 2048-point FIR filter designed by applying a Hamming window to an ideal LPF with cutoff at  $\pi/2$ . The sampling rate is fixed to  $\mu = 1/3 < 1/2$ . Thus, there is aliasing.

$N = 250,000$  samples of the additive error before filtering with  $H(\omega)$ ,  $w[n] = x[n]r_0[n]$ , are generated for each test case. Periodogram averaging with a Hamming window of size 1024 with 50% overlap is used to approximate 1024 samples of the power spectrum  $S_{ee}(\omega)$ . This estimate is summed and normalized to calculate the empirical MSE.

Fig. 2(a) shows the result of uniform sampling at rate  $\mu = 1/3$ . Note the strong aliases in the band of interest.

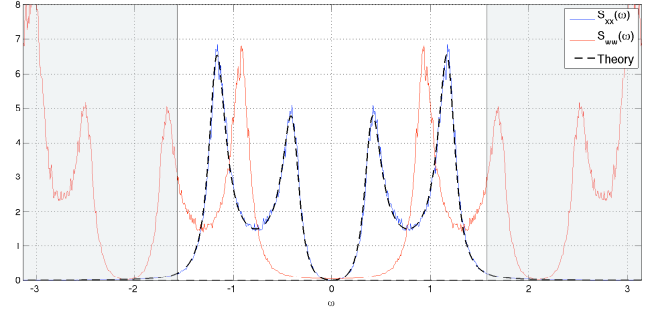
Fig 2(b) shows the result of SRS sampling with a white process of rate  $\mu = 1/3$ . As predicted, the noise has a flat power spectrum.

Fig 2(c) shows the result of non-white SRS sampling with two-pole binary AR process. The sampling process is generated according to the model of [8], with parameters  $a_1 = -0.1232$  and  $a_2 = 0.7505$ . These values are found through numerical optimization of Eqn.(11) for this specific  $H(\omega)$  and  $S_{xx}(\omega)$ . Note how the noise has been shaped out of band, so that the MSE is reduced beyond both white SRS and aliased uniform sampling.

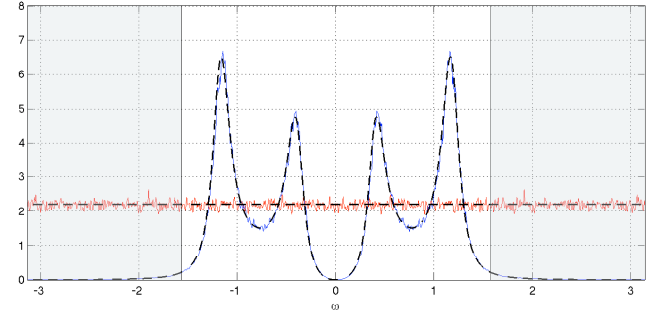
Fig 2(d) shows the result of DFW-FRS using the optimal MSE filters. The filters of Eqns.(24) and (25) are approximated using a 2048-tap FIR filter, computed using the inverse DFT of the sampled spectra of  $S_{xx}(\omega)$  and  $H(\omega)$ . For this example, the DFW-FRS MSE is lower than that of white SRS, but not as low as non-white SRS using a two-pole binary AR sampling process.

## 6. REFERENCES

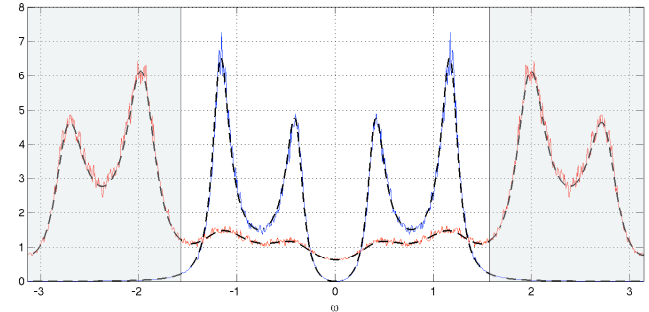
- [1] R. L. Cook, "Stochastic sampling in computer graphics," *ACM Transactions on Graphics*, vol. 5, no. 1, pp. 51–72, Jan 1986.
- [2] M. Said and A.V. Oppenheim, "Discrete-time randomized sampling," ICECS, Sept 2001.
- [3] M. Dippe and E. H. Wold, "Antialiasing through stochastic sampling," SIGGRAPH, July 1985, pp. 69–78.
- [4] D. P. Mitchell, "Generating antialiased images at low sampling densities," *Computer Graphics*, vol. 21, no. 4, pp. 65–72, July 1987.
- [5] I. Bilinkis and A. Mikelsons, *Randomized Signal Processing*, Prentice-Hall, 1992.
- [6] J.L. Martins de Carvalho and J.M.C. Clark, "Characterizing the autocorrelations of binary sequences," *IEEE Transactions on Information Theory*, vol. IT-29, no. 4, July 1983.
- [7] K.X. Karakostas and H.P. Wynn, "On the covariance function of stationary binary sequences with given mean," *IEEE Transactions on Information Theory*, vol. 39, no. 5, Sept 1993.
- [8] P. Boufounos, "Generating binary processes with autoregressive spectra," ICASSP, April 2007.



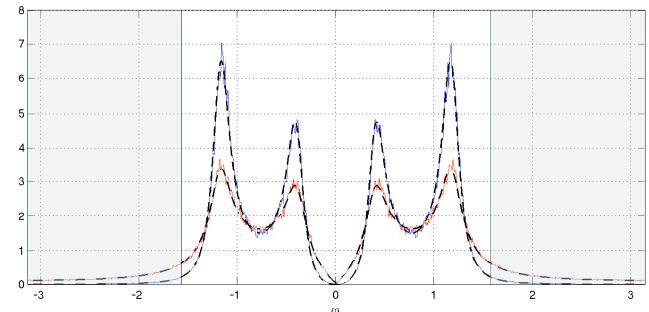
(a) Uniform. Emp. MSE = 5.02, Theor. MSE = 5.02



(b) White SRS. Emp. MSE = 6.94 , Theor. MSE = 6.89



(c) Binary AR SRS. Emp. MSE = 3.59 , Theor. MSE = 3.54



(d) Optimal FRS. Emp. MSE = 5.50 , Theor. MSE = 5.49

**Fig. 2.** Randomized sampling with  $S_{xx}(z)$  defined in Eqn.(27) and average sampling rate fixed to  $\mu = 1/3$ . Empirical and theoretical plots of  $S_{xx}(\omega)$  are shown. Empirical and theoretical plots of  $S_{ww}(\omega)$ , the error spectra before filtering with  $H(\omega)$ , are shown. Gray regions denote the stop-band of  $H(\omega)$ . White regions denote the pass-band of  $H(\omega)$ . The MSE is the area of the error power spectrum in the white region.